# Bayesian phase difference estimation algorithm for direct calculation of fine structure splitting: accelerated simulation of relativistic and quantum many-body effects

IOP Publishing Electron. Struct. 5 (2023) 035006 https://doi.org/10.1088/2516-1075/acf909

Electronic Structure



OPEN ACCESS

RECEIVED
14 April 2023

REVISED
8 August 2023

ACCEPTED FOR PUBLICATION
12 September 2023

PUBLISHED
25 September 2023



PAPER

# Bayesian phase difference estimation algorithm for direct calculation of fine structure splitting: accelerated simulation of relativistic and quantum many-body effects

**Kenji Sugisaki[1,2,3,*], V S Prasannaa[3], Satoshi Ohshima[4], Takahiro Katagiri[5], Yuji Mochizuki[6,7], B K Sahoo[8] and B P Das[3,9,*]**

[1] Graduate School of Science and Technology, Keio University, 7-1 Shinkawasaki, Saiwai-ku, Kawasaki, Kanagawa 212-0032, Japan
[2] Quantum Computing Center, Keio University, 3-14-1 Hiyoshi, Kohoku-ku, Yokohama, Kanagawa 223-8522, Japan
[3] Centre for Quantum Engineering, Research and Education (CQuERE), TCG Centres for Research and Education in Science and Technology (TCG CREST), Sector V, Salt Lake, Kolkata 700091, India
[4] Research Institute for Information Technology, Kyushu University, 744 Motooka, Nishi-ku, Fukuoka 819-0395, Japan
[5] Information Technology Center, Nagoya University, Furo-cho, Chikusa-ku, Nagoya, Aichi 464-8601, Japan
[6] Department of Chemistry, Faculty of Science, Rikkyo University 3-34-1 Nishi-ikebukuro, Toshima-ku, Tokyo 171-8501, Japan
[7] Institute of Industrial Science, The University of Tokyo, 4-6-1 Komaba, Meguro-ku, Tokyo 153-8505, Japan
[8] Atomic, Molecular and Optical Physics Division, Physical Research Laboratory, Navrangpura, Ahmedabad 380009, India
[9] Department of Physics, School of Science, Tokyo Institute of Technology, 2-12-1 Ookayama, Meguro-ku, Tokyo 152-8550, Japan
[*] Authors to whom any correspondence should be addressed.

**E-mail:** ksugisaki@keio.jp and bhanu.das@tcgcrest.org

**Keywords:** quantum computing, quantum algorithm, electronic structures, relativistic effects

Supplementary material for this article is available online

## Abstract

Despite rapid progress in the development of quantum algorithms in quantum computing as well as numerical simulation methods in classical computing for atomic and molecular applications, no systematic and comprehensive electronic structure study of atomic systems that covers almost all of the elements in the periodic table using a single quantum algorithm has been reported. In this work, we address this gap by implementing the recently-proposed quantum algorithm, the Bayesian phase difference estimation (BPDE) approach, to determine fine structure splittings of a wide range of boron-like atomic systems. Since accurate estimate of fine structure splittings strongly depend on the relativistic as well as quantum many-body effects, our study can test the potential of the BPDE approach to produce results close to the experimental values. Our numerical simulations reveal that the BPDE algorithm, in the Dirac–Coulomb–Breit framework, can predict fine structure splittings of ground states of the considered systems quite precisely. We performed our simulations of relativistic and electron correlation effects on Graphics Processing Unit by utilizing NVIDIA's cuQuantum, and observe a $\times 42.7$ speedup as compared to the Central Processing Unit-only simulations in an 18-qubit active space.

## 1. Introduction

Quantum computing and quantum information processing are currently among the fastest growing areas of research in modern science. In particular, recent rapid progress in the development of quantum hardware such as proof-of-principle experiments of surface code quantum error correction [1–3] motivates us to anticipate fault-tolerant quantum computing (FTQC) in the future. Among the wide landscape of diverse topics in quantum computing, sophisticated *ab initio* electronic structure calculations of atoms and molecules on quantum computers have especially attracted much attention due to their promising real-world applications [4–6]. Aiming for practical quantum computations, proper choice of a versatile quantum algorithm that can treat both light and heavy elements in the periodic table on the same footing is of crucial importance. The total energy of an atom or an atomic ion increases with atomic number. The variational quantum eigensolver [7, 8] is one of the most extensively studied algorithms for quantum

chemical calculations on near-term quantum devices, but its ability to predict energies of heavier systems with a sufficiently small standard deviation is limited by a massive increase in the measurement cost. In contrast, quantum phase estimation (QPE)-based approaches [9–12] are able to compute total energies of atoms and molecules with nearly constant measurement overhead regardless of the magnitude of total energies, although development of sophisticated theoretical methods to produce wave functions accurately even with reasonable approximation in a method is necessary [13–16]. The quantum circuit for QPE is usually too deep to execute on a noisy intermediate-scale quantum device, but QPE is anticipated to be a powerful tool for electronic structure calculations of atoms and molecules in the FTQC era. A systematic study of the electronic structure of atoms and atomic systems with different atomic numbers entails accounting for the relativistic effects, since the associated physical effects become prominent for the heavier elements. It is worth noting that even for the lighter atoms, physical phenomena that originates due to relativistic effects, such as the fine structure splitting, can be experimentally measured. However, most of the quantum simulations for quantum chemical calculations reported so far employ a non-relativistic Hamiltonian, and works in literature that take into account relativistic effects are still quite limited [17–21].

In this backdrop, we report numerical quantum simulations for the direct calculation of fine structure splitting of boron (B) isoelectronic sequence ($5 \leqslant Z \leqslant 103$, where Z is the atomic number of the considered system) by using a Bayesian phase difference estimation (BPDE) algorithm in conjunction with the four-component relativistic Dirac–Coulomb and Dirac–Coulomb–Breit Hamiltonians. Fine structure splitting is, as discussed below in detail, a purely relativistic effect and is affected by electron correlation, and therefore sophisticated treatments of both relativistic and correlation effects are necessary to calculate it quantitatively [22–28]. Since experimental fine structure splittings of wide variety of isoelectronic ions have been reported [29], they are good testing grounds for the sophisticated quantum chemical calculations on a quantum computer. The BPDE algorithm, which is recently proposed by one of the authors of the current work [30–32], is a general quantum algorithm for the direct calculation of energy gaps at the full configuration interaction (FCI) level of theory and it is suitable to compute small energy differences of systems with large total energies using a quantum computer. Since the BPDE algorithm can calculate an energy gap at the FCI level within an active space in the smallest Trotter decomposition error limit, the quality of the energy gap calculated at the FCI and BPDE is in principle the same. Note that the FCI calculation on a classical computer is based on the diagonalization of the Hamiltonian matrix, and eigenvalues of the electronic states belonging to the same symmetry can be obtained simultaneously. As we discuss in detail below, fine structure splitting is the energy gap between the electronic states with the same orbital and spin angular momenta ($L$ and $S$) but different total angular momentum $J$. Calculation of fine structure splitting on a classical computer usually requires two separate CI calculations for two different $J$ values. Conventional QPE-based FCI approaches on a quantum computer can in general compute the total energy of only one state in a single run, and therefore two separate QPE calculations are required to evaluate the fine structure splitting. In contrast, the BPDE algorithm is designed to calculate the energy gap directly, thereby allowing one to calculate the fine structure splitting in a single execution. Accelerating the computation times for quantum simulations using state-of-the-art techniques is an extremely important factor in carrying out numerical simulations of nearly a hundred systems rapidly. In this context, graphics processing unit (GPU) based quantum circuit simulations will become increasingly important for verifying the accuracy of quantum algorithms and developing new methods. In this work, we report such an acceleration by utilizing GPU with NVIDIA's cuQuantum Software Developer Kit [33]. To the best of our knowledge, this is the first comprehensive study of electronic structures of isoelectronic atomic series those covers almost all elements in the periodic table using a quantum algorithm.

Fine structure splitting refers to the energy separation caused by the consequence of couplings between electron spin angular momentum, $S$, and the orbital angular momentum, $L$, corresponding to two atomic states with different values of the total angular momentum quantum number, $J$. As an example, the electronic configuration of the ground state of B atom ($Z = 5$) in the non-relativistic scheme is $(1s)^2(2s)^2(2p)^1$. However, in the relativistic case, the degeneracy in six $p$ spin-orbitals is lifted and they split into two $p_{j=1/2}$ and four $p_{j=3/2}$ spin-orbitals. As a result, the electronic states ${}^2P_{1/2} = (1s_{1/2})^2(2s_{1/2})^2(2p_{1/2})^1$ and ${}^2P_{3/2} = (1s_{1/2})^2(2s_{1/2})^2(2p_{3/2})^1$ have different energies. The experimental value for the fine structure splitting of B atom is 15.287 $cm^{-1}$ [34], while in boron-like tungsten ($W^{69+}$), the energy gap is $1.1802 \times 10^7$ $cm^{-1}$ [35] (about six orders of magnitude larger than that of B). As pointed out above, the fine structure splitting is a purely relativistic effect and is affected by electron correlation. The extent to which the fine structure splitting is affected by electron correlation depends on the choice of system as well as the chosen states [22, 36]. In the case of B-isoelectronic sequence, the correlation effects reduce in importance as we go from lighter to heavier ions, while for our choice of states for these systems (${}^2P_{1/2}$ and ${}^2P_{3/2}$), pair correlation effects are the most important. In particular, the two particle-two hole excitations that result in configurations such as $(1s_{1/2})^2(2p_{1/2})^1(2p_{3/2})^2$, $(1s_{1/2})^2(2p_{1/2})^2(2p_{3/2})^1$, and $(1s_{1/2})^2(2p_{3/2})^3$ are dominant.

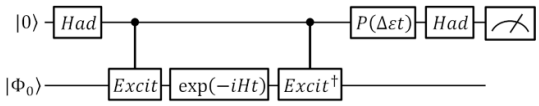


**Figure 1.** Quantum circuit for the BPDE algorithm. A probability of obtaining the $|0\rangle$ state in the measurement of the first qubit is provided in equation (4). The probability is maximized when $\Delta E = \Delta\varepsilon$, where $\Delta E$ is the energy gap of interest.

From the view point of quantum computation, a careful choice of systems such that their fine structure splittings span six orders of magnitude, followed by accurate determination of these quantities by a suitable quantum algorithm (BPDE in this case) would be a testament to the versatility of that algorithm.

## 2. Principle of BPDE

A typical quantum circuit for the BPDE algorithm is illustrated in figure 1. Here, we have used the notation '*Had*' for the Hadamard gate to distinguish it from the Hamiltonian, $H$. $P(\Delta\varepsilon t)$ is a phase rotation gate defined as

$$P(\Delta\varepsilon t) = \begin{pmatrix} 1 & 0 \\ 0 & e^{i\Delta\varepsilon t} \end{pmatrix}, \tag{1}$$

where $\Delta\varepsilon$ is used as the estimator of the energy gap and $t$ is the length of the time evolution. $|\Phi_0\rangle$ in figure 1 is an approximated wave function for the ground state that can be generated by using a shallow quantum circuit. An approximated excited state wave function $|\Phi_1\rangle$ is generated by applying a shallow *Excit* circuit to $|\Phi_0\rangle$. As discussed below, in the present calculations the quantum circuit for the generation of $|\Phi_0\rangle$ consists of five Pauli-X gates, and the controlled-*Excit* circuit is realized by two CNOT gates. These approximated wave functions can be expanded in the basis of eigenfunctions $\{|\Psi\rangle\}$ as

$$|\Phi_0\rangle = \sum_j c_j |\Psi_j\rangle \tag{2}$$

and

$$|\Phi_1\rangle = \sum_k d_k |\Psi_k\rangle, \tag{3}$$

where $c_j$ and $d_k$ are the corresponding expansion coefficients. Using equations (2) and (3), the probability of measuring the $|0\rangle$ state, Prob(0), in the quantum circuit depicted in figure 1 is calculated as

$$\mathrm{Prob}\,(0) = \frac{1}{2}\left[1 + \sum_{j,k} |c_j|^2 |d_k|^2 \cos\left\{\left(\Delta E_{jk} - \Delta\varepsilon\right) t\right\}\right]. \tag{4}$$

From equation (4), if the approximated wave functions have sufficiently large overlap with the eigenfunction of corresponding target states, Prob(0) becomes maximum around the point where $\Delta\varepsilon$ equals the energy difference between the two targeted states. Thus, we can calculate the energy gap by finding that value of $\Delta\varepsilon$ that gives maximum Prob(0). In the BPDE algorithm, $\Delta\varepsilon$ is optimized by means of Bayesian inference in the following procedure. (I) Define a prior distribution $Pr(\Delta\varepsilon)$ by a Gaussian function, in which the mean, $\mu$, corresponds to an initial estimate of the energy gap with a standard deviation $\sigma$. Note that $\sigma$ determines the energy range of the Bayesian search, and it should be large enough so that true $\Delta E$ locates between $(\mu - \sigma)$ and $(\mu + \sigma)$. (II) Repeatedly execute the quantum circuit in figure 1 with a fixed evolution time $t = 1.8/\sigma$ and different $\Delta\varepsilon$ in the range between $(\mu - \sigma)$ and $(\mu + \sigma)$ and generate the $\Delta\varepsilon$ vs. Prob(0) plot. Then, the plot is fitted by a Gaussian function and is used as a likelihood function $\Pr(0|\Delta\varepsilon; t)$. (III) Calculate a posterior distribution $\Pr(\Delta\varepsilon|0; t)$ using the equation

$$\Pr\left(\Delta\varepsilon|0;t\right) = \frac{Pr\left(0|\Delta\varepsilon;t\right)\Pr\left(\Delta\varepsilon\right)}{\int \Pr\left(0|\Delta\varepsilon;t\right)\Pr\left(\Delta\varepsilon\right) d\left(\Delta\varepsilon\right)}. \tag{5}$$

Since both $Pr(0|\Delta\varepsilon; t)$ and $\Pr(\Delta\varepsilon)$ are given as Gaussian functions, we can easily compute the posterior distribution. (IV) If the standard deviation of $\Pr(\Delta\varepsilon|0; t)$ is smaller than the convergence threshold $E_{\mathrm{Thre}}$, then return the mean of $\Pr(\Delta\varepsilon|0; t)$ as the estimate of $\Delta E$. Otherwise return to step (II) using the posterior distribution as the prior distribution in the next iteration.

## 3. Method of computation

The time evolution of wave functions is implemented using conventional techniques as follows. The second-quantized electronic Hamiltonian, built out of creation and annihilation operators (denoted below by $a^\dagger$ and $a$ respectively, and with their indices $p$, $q$, $r$, and $s$ running over the chosen single particle basis), is given by

$$H = \sum_{pq} h_{pq} a_p^\dagger a_q + \frac{1}{2} \sum_{pqrs} g_{pqrs} a_p^\dagger a_q^\dagger a_s a_r \tag{6}$$

and is transformed to a qubit Hamiltonian, which then takes the form

$$H = \sum_j w_j \left(\sigma_{N-1} \otimes \sigma_{N-2} \otimes \cdots \sigma_0\right), \sigma \in \{I, X, Y, Z\}, \tag{7}$$

using the Jordan–Wigner transformation [37]. In the equations (6) and (7), $h_{pq}$ and $g_{pqrs}$ refer to the one- and two- electron integrals, while in the qubit Hamiltonian, $w_j$ refers to the pre-factors for each of the terms in the transformed Hamiltonian, with each $w_j$ being a product of either a one- or a two- electron integral and a multiplicative factor resulting from the transformation itself. Subsequently, the quantum circuit corresponding to the time evolution operators is constructed [38] using second-order Trotter–Suzuki decomposition [39–41].

In the present study, we tested two different Hamiltonians: $H_{\mathrm{DC}}$ and $H_{\mathrm{DC+B}}$. $H_{\mathrm{DC}}$ is the Dirac–Coulomb Hamiltonian, defined by the equation (in atomic units (a.u.))

$$H_{\mathrm{DC}} = \sum_i \left[c\boldsymbol{\alpha}_i \cdot \mathbf{p}_i + (\beta_i - 1)c^2 + V_n(r_i)\right] + \sum_{j>i} \frac{1}{r_{ij}}, \tag{8}$$

while $H_{\mathrm{DC+B}}$ contains an additional term, $V_{\mathrm{B}}$, given by

$$V_{\mathrm{B}} = -\sum_{j>i} \left\{ \frac{\boldsymbol{\alpha}_i \cdot \boldsymbol{\alpha}_j}{2r_{ij}} + \frac{(\boldsymbol{\alpha}_i \cdot \mathbf{r}_{ij})(\boldsymbol{\alpha}_j \cdot \mathbf{r}_{ij})}{2r_{ij}^3} \right\} \tag{9}$$

to take into account the full Breit interaction in addition to $H_{\mathrm{DC}}$. In the above equations, $c$ is the speed of light, $\boldsymbol{\alpha}$ and $\beta$ are the $4 \times 4$ Dirac matrices, $\mathbf{p}_i$ is the momentum operator associated with the $i^{\mathrm{th}}$ electron, $V_n(r_i)$ is the electron–nucleus potential, and $1/r_{ij}$ is the electron–electron Coulomb interaction term (in a.u.). A recent theoretical study by Wan and coworkers showed that relative contributions of Breit interactions to the fine structure splitting of B-isoelectronic sequence are significant for light elements, and is as large as 14.55% for neutral boron [28].

For the accurate computation of fine structure splitting, it is important to treat the $^2P_{1/2}$ ground state and the $^2P_{3/2}$ excited state on an equal footing [22]. In this work, the one- and two-electron integrals were computed at the Dirac–Fock level for the state with one electron removed from the corresponding target systems ($B^+$ and its isoelectronic sequence) using our own in-house code. Gaussian-type universal basis ($\alpha_0 = 0.01$ and $\beta = 1.80$) with 40 $s_{1/2}$, 39 $p_{1/2}$, and 39 $p_{3/2}$ orbitals is used for the Dirac–Fock calculations. The large and the small components of Dirac–Fock orbitals are kinetically balanced [42]. In the BPDE simulations, we tested two types of active spaces; (1s, 2s, 2p) with 10 qubits and (1s, 2s, 2p, 3s, 3p) with 18 qubits, without adopting any qubit tapering techniques. Note that two-qubit tapering based on electron number conservation rule in the parity basis and the symmetry-conserving Bravyi–Kitaev transformation [43] assumes non-relativistic calculations in which the electron spin quantum number is a good quantum number. Applying these techniques to relativistic calculations is not straightforward. Throughout this paper, when we use, for example, the notation (18q, $H_{\mathrm{DC+B}}$), it specifies the active space and Hamiltonian being used.

We now comment on the effect of Trotter error on our results. It is known that Trotter decomposition error depends on the maximum atomic charge of a system [44], and therefore finer Trotter decomposition should be employed for heavier elements. In the present study, we set the time length of a single Trotter step as $t/M = \min[0.2, 10/|h_{00}|]$, where $M$ is the number of Trotter slices and $h_{00}$ is the one-electron integral corresponding to electron–nuclear attraction of the $1s_{1/2}$ electrons. We used single Slater determinant wave functions for the approximated wave functions of the $^2P_{1/2}$ and the $^2P_{3/2}$ states: $|\Phi_0\rangle = |(1s_{1/2})^2(2s_{1/2})^2(2p_{1/2})^1\rangle$ and $|\Phi_1\rangle = |(1s_{1/2})^2(2s_{1/2})^2(2p_{3/2})^1\rangle$, respectively. In this case, $|\Phi_0\rangle$ is prepared by using five Pauli-X gates, and the controlled-*Excit* circuit in figure 1 is realized by two CNOT gates. The difference between the energy expectation values of two approximated wave functions is used as

the initial mean of the prior distribution: $\mu_{\rm ini} = \Delta E_{\rm Ref} = \langle\Phi_1|H|\Phi_1\rangle - \langle\Phi_0|H|\Phi_0\rangle$, and the initial standard deviation of the prior distribution is set as $\sigma_{\rm ini} = \max[0.1, 10|\mu_{\rm ini}|]$ in units of hartree. In step (II) of the BPDE algorithm, we draw 21 samples in the range of $(\mu - \sigma)$ to $(\mu + \sigma)$ with a constant interval, and execute the quantum circuit 5000 times for each sample to construct the likelihood function. The convergence threshold for Bayesian optimization in the step (IV) is set to be inversely proportional to the time of a single Trotter step, $E_{\rm Thre} = 0.001M/t$ hartree. These computational conditions were selected to calculate the fine structure splitting of B-isoelectronic sequence with similar computational costs regardless of the atomic number Z. Using these conditions, the number of Trotter slices, $M$, in the final iteration is about 1000 for all atoms being studied.

The numerical simulation program for the BPDE algorithm was developed using Python3 with OpenFermion [45], Cirq [46], and cuQuantum [33] libraries. To execute numerical simulations with GPU acceleration, we prepared the simulation environment on a Supercomputer 'Flow' Type II subsystem in Nagoya University. The 'Flow' Type II subsystem consists of the FUJITSU Server PRIMERGY CX2570 M5, including the Intel Xeon Gold 6230 with 20 cores × 2 sockets, and the NVIDIA Tesla V100 (Volta) × 4 GPUs, thus 33.888 TFLOPS in a node. 384 GiB (DDR4 2933 MHz) memory, and 6.4TB/node SSD in each node are available. In addition, local shared storage (BeeGFS, BeeOND, NVMesh) is also provided. The total number of nodes is 221, and hence total FLOPS is 33.888 TFLOPS × 221 nodes = 7.489 PFLOPS. The numerical simulations for 10 qubit active space were executed on Linux workstations without GPU accelerations, and those for 18 qubit active space were carried out on 'Flow' Type II subsystem. Because the BPDE algorithm computes the likelihood function based on statistical sampling of the measurement outcome, the algorithm returns different values for every run. In this study, all the numerical simulations were carried out five times. The standard deviations of five runs for B are about 0.7–2.0 $\rm cm^{-1}$, and those for boron-like ions (99 atoms in total) are on average 199.8, 163.2, 136.3, and 167.7 $\rm cm^{-1}$ for (10q, $H_{\rm DC}$), (18q, $H_{\rm DC}$), (10q, $H_{\rm DC+B}$), and (18q, $H_{\rm DC+B}$), respectively, and they are sufficiently small compared to the calculated values of $\Delta E_{\rm BPDE}$.

## 4. Results and discussion

The fine structure splitting values obtained from the numerical simulations of the BPDE algorithm using (18q, $H_{\rm DC+B}$) as well as the experimental values [29] are plotted in figure 2(a), and the ratios $\Delta E_{\rm BPDE}/\Delta E_{\rm Exptl}$ and $\Delta E_{\rm BPDE}/\Delta E_{\rm CASCI}$ are given in figures 2(b) and (c), respectively. Note that CASCI is the acronym for complete active space configuration interaction, and it corresponds to the FCI treatment within the selected active orbitals. All the calculated fine structure splitting values are provided in the supplemental material. For light elements, deviation of the $\Delta E_{\rm BPDE}$ values from experimental ones appears to be large, but this observation is a consequence of the fine structure splitting being small. In fact, the fine structure splitting of B calculated using the BPDE algorithm with (18q, $H_{\rm DC+B}$) is $\Delta E = 12.5287 \pm 0.9813$ $\rm cm^{-1}$, and the absolute error with respect to the experimental value is only about 3 $\rm cm^{-1}$. Another possible reason for the significant deviation of $\Delta E_{\rm BPDE}/\Delta E_{\rm Exptl}$ values from 1 for low-Z elements is related to the quality of the approximated wave functions. As we discussed in section 2, the peak position of the likelihood function can be shifted in the presence of contributions from electronic states other than the target states. Electron correlation effects are more significant and the overlap squared values $|\langle\Phi_0|\Psi_0\rangle|^2$ and $|\langle\Phi_1|\Psi_1\rangle|^2$ are smaller for low-Z elements. This means that the contributions other than the $|c_0|^2|d_1|^2\cos\{(\Delta E_{01} - \Delta\varepsilon)t\}$ term in the right hand side of equation (4) are not negligible for low-Z elements, which can affect the estimated energy gaps $\Delta\varepsilon$. For example, the calculated $|c_0|^2$ and $|d_1|^2$ values of B atom are 0.9335 and 0.9334, respectively, but those of $Lr^{98+}$ are 0.9999 and 0.9919, respectively. However, the $\Delta E$ value of B obtained from the BPDE simulations is very close to that calculated at the CASCI level (12.2715 $\rm cm^{-1}$), and therefore departure of the $\Delta E_{\rm BPDE}$ value from the experimental one cannot be fully explained by the quality of the approximated wave functions. The most reasonable explanation for the deviation of $\Delta E_{\rm BPDE}/\Delta E_{\rm Exptl}$ from 1 is the limited active space size. In particular, absence of the 3d orbitals in the active space may lead to an insufficient description of angular correlation [47], which is expected to be important for low-Z elements. We expect that inclusion of more virtual orbitals (3d, 4s, 4p, and above) can further improve the accuracy of the fine structure splitting. Note that all the $\Delta E_{\rm BPDE}/\Delta E_{\rm CASCI}$ values (figure 2(c)) are in the range 0.92 and 1.05, thus indicating the ability of the BPDE algorithm in being able to reproduce the CASCI fine structure splitting very accurately.

The agreement in the values of $\Delta E_{\rm BPDE}$ with $\Delta E_{\rm Exptl}$ in highly charged ions is also worth emphasizing. In this context, we note that for heavier ions, relativistic effects are dominant and electron correlation effects becomes less significant. Nevertheless, the fine structure splittings computed by using the BPDE algorithm are closer to the experimental values than those estimated from the reference wave functions $\Delta E_{\rm Ref}$. For example, the fine structure splitting in boron-like tungsten ($W^{69+}$) is calculated to be $\Delta E_{\rm Ref} = 11,841,730$ $\rm cm^{-1}$ and $\Delta E_{\rm BPDE} = 11,800,183$ $\rm cm^{-1}$ for (18q, $H_{\rm DC+B}$), and the experimental value is $\Delta E_{\rm Exptl} = 11,802,000$ $\rm cm^{-1}$. These results also exemplify the capability of the BPDE algorithm in predicting

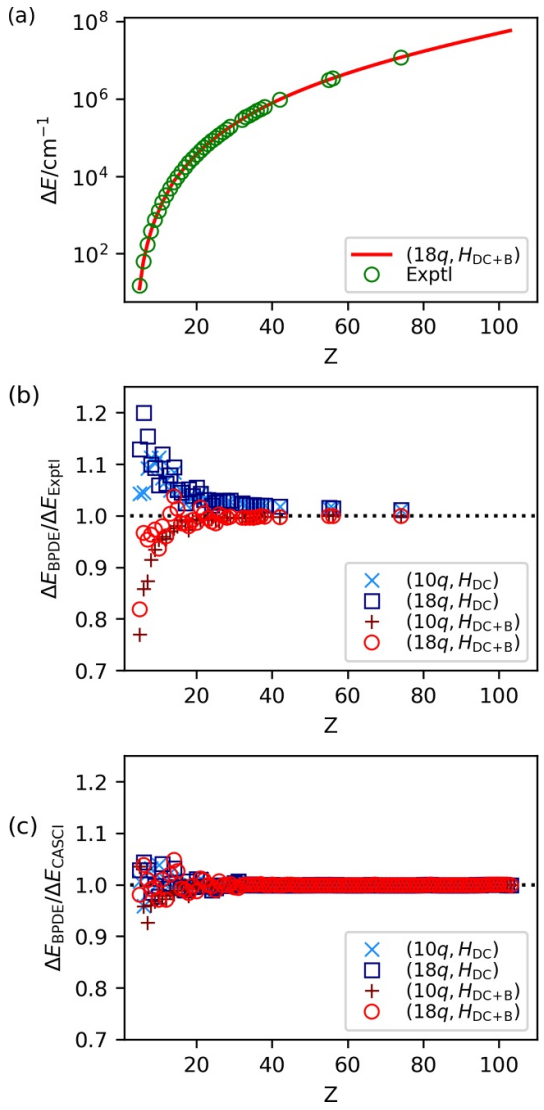


**Figure 2.** Results of numerical simulations of the BPDE-based fine structure splitting calculations. (a) The fine structure splitting values calculated by the BPDE algorithm using (18q, $H_{\mathrm{DC+B}}$) (red line) and experimental values (green circles). (b) The $\Delta E_{\mathrm{BPDE}}/\Delta E_{\mathrm{Exptl}}$ values. (c) The $\Delta E_{\mathrm{BPDE}}/\Delta E_{\mathrm{CASCI}}$ values.

**Table 1.** The root mean square deviations of the $\Delta E_{\mathrm{BPDE}}$ from $\Delta E_{\mathrm{Exptl}}$.

| Hamiltonian | Size of active space | RMSD/cm$^{-1}$ |
|---|---|---|
| $H_{\mathrm{DC}}$ | 10 | 9966.6 |
| $H_{\mathrm{DC}}$ | 18 | 10 139.7 |
| $H_{\mathrm{DC+B}}$ | 10 | 698.0 |
| $H_{\mathrm{DC+B}}$ | 18 | 605.3 |

the energy gap accurately. The root mean square deviations of the $\Delta E_{\mathrm{BPDE}}$ from $\Delta E_{\mathrm{Exptl}}$ were summarized in table 1. It is worth noting that the agreement with the experimental values drastically improved by considering the Breit interaction, and the larger active space with more sophisticated Hamiltonian (18q, $H_{\mathrm{DC+B}}$) gives the best agreement.

In order to check for GPU acceleration in our numerical quantum circuit simulation, we executed the BPDE calculations of boron fine structure splitting with 8, 10, 16, and 18 qubit active spaces in conjunction with $H_{\mathrm{DC+B}}$ on our Linux workstation (CPU: Intel Xeon-Gold 6134, GPU: None) and 'Flow' Type II subsystem (CPU: Intel Xeon-Gold 6230, GPU: NVIDIA Tesla V100). The 8 and 16 qubit active spaces were prepared by fixing the occupation number of $1s_{1/2}$ orbitals in the 10 and 18 qubit active spaces, respectively. For 8 and 10 qubit active spaces, we also carried out the BPDE simulations on 'Flow' Type II subsystem without using GPU. All the simulations were performed five times using single thread.

**Table 2.** Average time taken for BPDE quantum circuit simulation for B atom fine structure splitting, in units of seconds.

| | | 'Flow' Type II[b] | |
|---|---|---|---|
| Size of active space | Workstation[a] w/o GPU | w/o GPU | with GPU |
| 8 | 628 | 731 | 177 |
| 10 | 2197 | 2267 | 588 |
| 16 | 73 452 | — | 4830 |
| 18 | 387 328 | — | 9081 |

[a] CPU: Intel Xeon-Gold 6134, GPU: None.
[b] CPU: Intel Xeon-Gold 6230, GPU: NVIDIA Tesla V100.

The average simulation time of five runs are given in table 2. From the table, the speedup in GPU-accelerated quantum circuit simulations is significant, especially when a larger active space is employed. For smaller active spaces (8q and 10q), the speedup is about $\times 4$. By contrast, for 16 and 18 qubit active spaces, GPU-based simulations provide substantial speedups of 15.2 and 42.7 times, respectively. Note that the computation times of both CPU and GPU-based quantum circuit simulations scales exponentially with the number of qubits, but the exponent is smaller for GPU than CPU. It is worth noting that that all simulations were completed within a week by using a supercomputer with GPUs, whereas executing all calculations solely on workstations without GPUs will take about a year.

## 5. Summary

Our numerical quantum simulations show that the fine structure splitting of the boron isoelectronic sequence can be computed very accurately by appropriately considering both relativistic and quantum many-body effects using the BPDE algorithm. By using the (1s, 2s, 2p, 3s, 3p) active space and the relativistic Dirac–Coulomb–Breit Hamiltonian, the fine structure splittings in boron isoelectronic sequence were predicted within 605.3 $cm^{-1}$ of the root mean square deviation from the experimental values. This root mean square deviation value is the smallest among the four cases involving different combinations of Hamiltonian and number of qubits that we tested. It is noteworthy that the deviations in the calculated fine structure splittings from the experimental values do not increase nearly as much as they do with increase in atomic number. Two of our important findings in this work regarding accuracy of the calculated fine structure splitting are (a) that it is crucial to include Breit interactions for accurate predictions of fine structure splittings for the systems that we have considered, and (b) that it is necessary to include virtual orbitals to improve our results for the lighter systems (neutral boron and the lighter boron-like ions). Considering the fact that the BPDE algorithm is a FTQC or an early-FTQC algorithm, it is quite challenging to run the BPDE algorithm on today's real quantum hardware. Recently, the BPE-based FCI calculations of $H_2$ molecule using an ion trap quantum processor have been reported [48]. Since the BPDE algorithm is free of the controlled-time evolution operation that is necessary for conventional BPE algorithm, BPDE is potentially more suitable for hardware executions than BPE. However, as we discussed in section 3, two-qubit tapering technique is generally not applicable to relativistic quantum chemical calculations. Sophisticated quantum circuit optimizations [49, 50] to reduce the depth of the circuit and the number of two-qubit gates are necessary for proof-of-principle demonstrations of the BPDE-based fine structure splitting calculations on a quantum computer, even if we use small active space. Speedup in numerical simulations of quantum circuits by using GPU in conjunction with NVIDIA cuQuantum is significant, especially when large active space is employed. We observed $\times 42.7$ speedup for 18-qubit active space simulations. Such acceleration of quantum circuit simulations is important to test the ability of the quantum algorithms to handle problems of larger size, for further development of quantum algorithms for various applications.

## Data availability statement

The data that support the findings of this study are available upon reasonable request from the authors.

## Acknowledgments

The authors thank Shinya Morino (NVIDIA Japan) for helpful discussions on the cuQuantum simulation environment construction on 'Flow' Type II subsystem. This work was supported by JST PRESTO 'Quantum Software' Project (Grant No. JPMJPR1914), Japan and KAKENHI Scientific Research C (Grant No. 21K03407) from JSPS, Japan. The computation was carried out using the JHPCN Joint Research Projects (jh220010) on supercomputer 'Flow' at Information Technology Center, Nagoya University. K Sugisaki

acknowledges the partial support from the Center of Innovations for Sustainable Quantum AI (Grant No. JPMJPF2221) from JST, Japan, Quantum Leap Flagship Program (JPMXS0120319794) from the MEXT, Japan, and KAKENHI Transformative Research Area B (23H03819) from JSPS, Japan. Y Mochizuki acknowledges the support from Rikkyo SFR.

## ORCID iDs

Kenji Sugisaki https://orcid.org/0000-0002-1950-5725
V S Prasannaa https://orcid.org/0000-0002-5115-9295
Satoshi Ohshima https://orcid.org/0000-0003-4073-5688
Takahiro Katagiri https://orcid.org/0000-0001-7193-9304
Yuji Mochizuki https://orcid.org/0000-0002-7310-5183
B K Sahoo https://orcid.org/0000-0003-4397-7965

## References

[1] Krinner S *et al* 2022 Realizing repeated quantum error correction in a distance-three surface code *Nature* **605** 669–74
[2] Zhao Y *et al* 2022 Realization of an error-correcting surface code with superconducting qubits *Phys. Rev. Lett.* **129** 030501
[3] Acharya R *et al* 2023 Suppressing quantum errors by scaling a surface code logical qubit *Nature* **614** 676–81
[4] Cao Y *et al* 2019 Quantum chemistry in the age of quantum computing *Chem. Rev.* **119** 10856–915
[5] Bauer B, Bravyi S, Motta M and Chan G K-L 2020 Quantum algorithms for quantum chemistry and quantum materials science *Chem. Rev.* **120** 12685–717
[6] Motta M and Rice J E 2022 Emerging quantum computing algorithms for quantum chemistry *WIREs Comput. Mol. Sci.* **12** e1580
[7] Peruzzo A, McClean J, Shadbolt P, Yung M-H, Zhou X-Q, Love P J, Aspuru-Guzik A and O'Brien J L 2014 A variational eigenvalue solver on a photonic quantum processor *Nat. Commun.* **5** 4213
[8] Tilly J *et al* 2022 The variational quantum eigensolver: a review of methods and best practices *Phys. Rep.* **986** 1–128
[9] Aspuru-Guzik A, Dutoi A D, Love P J and Head-Gordon M 2005 Simulated quantum computation of molecular energies *Science* **309** 1704–7
[10] Lanyon B P *et al* 2010 Towards quantum chemistry on a quantum computer *Nat. Chem.* **2** 106–11
[11] Du J, Xu N, Peng X, Wang P, Wu S and Lu D 2010 NMR implementation of a molecular hydrogen quantum simulation with adiabatic state preparation *Phys. Rev. Lett.* **104** 030502
[12] Bauman N P *et al* 2021 Toward quantum computing for high-energy excited states in molecular systems: quantum phase estimations of core-level states *J. Chem. Theory Comput.* **17** 201–10
[13] Veis L and Pittner J 2014 Adiabatic state preparation study of methylene *J. Chem. Phys.* **140** 214111
[14] Sugisaki K, Nakazawa S, Toyota K, Sato K, Shiomi D and Takui T 2019 Quantum chemistry on quantum computers: a method for preparation of multiconfigurational wave functions on quantum computers without performing Post–Hartree–Fock calculations *ACS Cent. Sci.* **5** 167–75
[15] Sugisaki K, Toyota K, Sato K, Shiomi D and Takui T 2022 Adiabatic state preparation of correlated wave functions with nonlinear scheduling functions and broken-symmetry wave functions *Commun. Chem.* **5** 84
[16] Halder D, Prasannaa V S, Agarawal V and Maitra R 2022 Iterative quantum phase estimation with variationally prepared reference state *Int. J. Quantum Chem.* **123** e27021
[17] Veis L, Višňák J, Fleig T, Knecht S, Saue T, Visscher L and Pittner J 2012 Relativistic quantum chemistry on quantum computers *Phys. Rev.* A **85** 030304(R)
[18] Zaytsev V A, Groshev M E, Maltsev I A, Durova A V and Shabaev V M 2023 Calculation of the moscovium ground-state energy by quantum algorithms *Int. J. Quantum Chem.* e27232
[19] Stetina T F, Ciavarella A, Li X and Wiebe N 2022 Simulating effective QED on quantum computers *Quantum* **6** 622
[20] Swain K R, Prasannaa V S, Sugisaki K and Das B P 2022 Calculation of molecular electric dipole moments of light and moderately heavy molecules using relativistic VQE algorithm (arXiv:2211.06907)
[21] Kumar V, Baskaran N, Prasannaa V S, Sugisaki K, Mukherjee D, Dyall K G and Das B P 2022 Accurate calculation of relativistic excitation energies using quantum annealing (arXiv:2212.01801)
[22] Das B P, Hata J and Grant I P 1984 Ground-state fine structure in the boron isoelectronic sequence *J. Phys. B: At. Mol. Phys.* **17** L1–L5
[23] Das B P, Latha K V P, Sahoo B K, Sur C, Chaudhuri R K and Mukherjee D 2005 Relativistic and correlation effects in atoms *J. Theor. Comput. Chem.* **4** 1–20
[24] Marques J P, Indelicato P and Parente F 2012 Relativistic multiconfiguration calculations of the $2s^2 2p^2 P_{3/2}$ level lifetime along the boron isoelectronic sequence *Eur. Phys. J.* D **66** 324
[25] Dutta N N and Majumder S 2012 *Ab initio* studies of electron correlation and Gaunt interaction effects in the boron isoelectronic sequence using coupled-cluster theory *Phys. Rev.* A **85** 032512
[26] Artemyev A N, Shabaev V M, Tupitsyn I I, Plunien G, Surzhykov A and Fritzsche S 2013 *Ab initio* calculations of the $2p_{3/2} - 2p_{1/2}$ fine-structure splitting in boronlike ions *Phys. Rev.* A **88** 032518
[27] Yu Y and Sahoo B K 2019 Investigating ground-state fine-structure properties to explore suitability of boronlike $S^{11+} - K^{14+}$ and galliumlike $Nb^{10+} - Ru^{13+}$ ions as possible atomic clocks *Phys. Rev.* A **99** 022513
[28] Wan J-J, Li J and Gu J 2021 Residual electronic correlation and QED effects in fine-structure splitting of ground configuration for the boron isoelectronic sequence *Result Phys.* **31** 105004
[29] Kramida A, Ralchenko Y and Reader J (NIST AST Team) 2022 NIST atomic spectra database (version 5.10) (National Institute of Standards and Technology) (https://doi.org/10.18434/T4W30F)
[30] Sugisaki K, Sakai C, Toyota K, Sato K, Shiomi D and Takui T 2021 Bayesian phase difference estimation: a general quantum algorithm for the direct calculation of energy gaps *Phys. Chem. Chem. Phys.* **23** 20152–62
[31] Sugisaki K, Sakai C, Toyota K, Sato K, Shiomi D and Takui T 2021 Quantum algorithm for full configuration interaction calculations without controlled time evolutions *J. Phys. Chem. Lett.* **12** 11085–9

[32] Sugisaki K, Wakimoto H, Toyota K, Sato K, Shiomi D and Takui T 2022 Quantum algorithm for numerical energy gradient calculations at the full configuration interaction level of theory *J. Phys. Chem. Lett.* **13** 11105–11
[33] Bayraktar H *et al* 2023 cuQuantum SDK: a high-performance library for accelerating quantum science (arXiv:2308.01999)
[34] Kraminda A E and Ryabtsev A N 2007 A critical compilation of energy levels and spectral lines of neutral boron *Phys. Scr.* **76** 544–57
[35] Clementson J, Beiersdorfer P, Brown G V, Gu M F, Lundberg H, Podpaly Y and Träbert E 2011 Tungsten spectroscopy at the Livermore electron beam ion trap facility *Can. J. Phys.* **89** 571–80
[36] Perger W F and Das B P 1987 Multiconfigurational Dirac-Fock calculations of fine-structure intervals in the beryllium isoelectronic sequence *J. Phys. B: At. Mol. Phys.* **20** 665
[37] Jordan P and Wigner E 1928 Über das Paulische äquivalenzverbot *Z. Phys.* **47** 631–51
[38] Whitfield J D, Biamonte J and Aspuru-Guzik A 2011 Simulation of electronic structure Hamiltonians using quantum computers *Mol. Phys.* **109** 735–50
[39] Trotter H F 1959 On the product of semi-groups of operators *Proc. Am. Math. Soc.* **10** 545–51
[40] Suzuki M 1976 Relationship between $d$-dimensional quantal spin systems and $(d+1)$-dimensional Ising systems: equivalence, critical exponents and systematic approximants of the partition function and spin correlations *Prog. Theor. Phys.* **56** 1454–69
[41] Hatano N and Suzuki M 2005 Finding exponential product formulas of higher orders *Quantum Annealing and Other Optimization Methods* (*Lecture Notes in Physics* vol 679), ed A Das and B K Chakrabarti (Springer) pp 37–68
[42] Dyall K G, Grant I P and Wilson S 1984 The dirac equation in the algebraic approximation. II. Extended basis set calculations for hydrogenic atoms *J. Phys.* B **17** L45
[43] Bravyi S, Gambetta J M, Mezzacapo A and Temme K 2017 Tapering off qubits to simulate fermionic Hamiltonians (arXiv:1701.08213)
[44] Babbush R, McClean J, Wecker D, Aspuru-Guzik A and Wiebe N 2015 Chemical basis of Trotter-Suzuki errors in quantum chemistry simulation *Phys. Rev.* A **91** 022311
[45] McClean J R *et al* 2020 OpenFermion: the electronic structure package for quantum computers *Quantum Sci. Technol.* **5** 034014
[46] Cirq Developers 2022 Cirq (Version v1.0.0) (available at: https://github.com/quantumlib/Cirq)
[47] Magnusson E 1993 The role of d functions in correlated wave functions: main group molecules *J. Am. Chem. Soc.* **115** 1051–61
[48] Yamamoto K, Duffield S, Kikuchi Y and Ramo D M 2023 Demonstrating Bayesian quantum phase esitmation with quantum error detection (arXiv:2306.16608)
[49] Kharkov Y, Ivanova A, Mikhantiev E and Kotelnikov A 2022 Arline benchmarks: automated benchmarking platform for quantum compilers (arXiv:2202.14025)
[50] Baskaran N, Rawat A S, Jayashankar A, Chakravarti D, Sugisaki K, Roy S, Mandal S B, Mukherjee D and Prasannaa V S 2022 Adapting the HHL algorithm to (non-unitary) quantum many-body theory (arXiv:2212.14781)